

NUMERICAL INVESTIGATIONS ON THE SLENDER AXISYMMETRIC BODIES AERODYNAMICS IN WIDE RANGE OF MACH NUMBERS AND ANGLES OF ATTACK FROM 0° TO 180°

N.V. Voevodenko*, L.G. Ivanteeva*, V.Ju. Lunin*
*** TsAGI – Central Aerohydrodynamic Institute, Russia**

Keywords: *numerical aerodynamics, high Mach and AoA*

Abstract

Numerical investigations of the aerodynamic characteristics and the flows around slender axisymmetric bodies in wide parameters range: $M_\infty=0. \div 10.$, $\alpha=0^\circ \div 180^\circ$ are considered. Various numerical, theoretical and engineering methods are applied to calculate aerodynamic characteristics of two buster configurations. The various methods applicability range is determined for this problem.

1 Introduction

The environment survivability and Earth ecology become more and more important now. The problem considered in this paper is directly connected with that. In various projects aimed at the high-velocities aircraft development the rocket busters are used to accelerate the vehicles. 10-20 years ago no one was interested, where the buster stages fall. But now on the desk of the aerospace engineers and scientists was putted the problem to determine the trajectory and the fall area of such objects. Similar problems are considered in different countries, for example, a number of experimental investigations, including flight experiments, have been conducted in USA to predict the places of the accelerator booster stage falls.

This paper challenge is to investigate the flow around slender axisymmetric bodies in wide range of Mach numbers and angles of attack. Normally, the buster stages are slender axisymmetric bodies, and it is necessary to know their aerodynamic characteristics to determine the place of their falls. The buster

stage discharge can be performed in the wide range of Mach numbers $M_\infty=0 \div 10$, and bodies themselves can round up in the fall and flight at arbitrary angles of attack - α , so it is necessary to determine their all-round flow at $\alpha=0^\circ \div 180^\circ$.

To solve the problem, mentioned above, authors have used a number of numerical, theoretical and engineering methods, described in part 2.

A number of numerical investigations have been conducted in the frame of this work to verify the applied methods validity. The studies have shown the possibility to use the approximate tools (for example, based on the hypersonic small disturbance theory – HSDT, or Newton's method), to solve the problem under consideration at high Mach numbers $M_\infty=1.5 \div 10$.

At low Mach numbers $M_\infty = 0. \div 2.$ approximate methods are non-applicable, due to their applicability restrictions and to the contribution of the leeward side flow, where strong vortexes are significant. In this range the RANS – solutions can be obtained with NUMECA, ANSYS CFX or similar CFD codes.

2 Methods of the problem solution

Due to the wide range of flow parameters $M_\infty=0 \div 10$, $\alpha=0^\circ \div 180^\circ$ it was not possible to use the same tool for whole range calculations. To solve the problem, mentioned above, authors have used a number of numerical, theoretical and engineering methods, including the following:

- CFD- codes ANSYS CFX and NUMECA are used to solve RANS equations at subsonic and low

supersonic velocities: $M_\infty=0\div 2$,
 $\alpha=0^\circ\div 180^\circ$;

- program package NINA, based on 1) Sychev's theory, which extends the hypersonic small disturbance theory (HSDT) to the high angles of attack range; 2) Godunov-Kolgan numerical method to solve 2D unsteady Euler equations, - at super- and hypersonic velocities: $M_\infty=1.5\div 10$, $\alpha=0^\circ\div 180^\circ$;

The wide range of flow parameters and the variety of the body shapes lead to the huge number of calculations. This is why quick and robust numerical and engineering tools are very useful for such calculations.

2.1 Method for high Mach numbers

For calculations at high Mach numbers, $M_\infty=1.5\div 10$ was used the numerical method (program package NINA), based on HSDT [1] and Sychev's theory [2].

HSDT was developed basing on following main assumptions:

$$M_\infty \gg 1, \quad \tau \sim \delta = \frac{d}{l} \ll 1, \quad K = M_\infty \tau \sim 1 \quad (1)$$

Here l is the body length, d is the maximum transverse dimension of the body, and δ is the relative body thickness, τ the relative disturbed layer thickness. HSDT assumes that angle of attack (AoA) is small and the relative disturbed layer thickness is small and of the same order as the relative body thickness.

Theory [2] considers the case of hypersonic flow around arbitrary slender body at an arbitrary AoA. It assumes that:

$$\delta \ll 1, \quad M_\infty \delta \geq 1, \quad M_\infty \sin \alpha \gg 1 \quad (2)$$

At small AoA - α theory [2] transforms to theory [1]. The most important parameter, characterizing the precision of theories [1] and [2] is a disturbed flow thickness τ , which should be of the same order as the body thickness, presumed to be small (slender body). This assumption is valid at high Mach numbers and small angles of attack α . But with the α rise the disturbed layer on the body leeward side is spread far from the body surface and the complex vortex flow, which

can't be modeled by the Euler equations, arises in this region. For all that, at high Mach numbers and high α the disturbed layer on windward side is thin, and the HSDT is valid. The situation is saved by the fact, that the flow parameters (pressure, density, temperature) values on the on windward side are much higher than ones on the leeward side. Therefore, the leeward side contribution is not significant in comparison with the windward side one.

HSDT and Sychev's theories reduce the 3D Euler equations and boundary conditions to 2D-t (two dimensional unsteady) Euler equations and boundary conditions. 2D-t problem is integrated by numerical method [3]. Package NINA (Numerical Investigations of Nonlinear Aerodynamics) is based on this complex of theoretical and numerical methods. It is described in detail in [4].

The small leeward side contribution is one of the basic assumptions in Sychev's theory and it was checked up by direct comparison of parameters, obtained in calculations, on both sides of the axisymmetric bodies. The results are presented below.

2.1.1 Methods assumptions verification

Numerical investigations have been conducted in the frame of this work to verify the applied methods assumptions validity, concerning small values of the leeward side flow parameters in comparison with the windward side ones. This assumption validation was performed by direct flow parameters comparison on the both sides. The flow field parameters have been calculated by NINA package and by ANSYS CFX and NUMECA codes, which solved RANS – equations with different turbulence models.

Flow parameter have been considered on the cylinder surface at fixed AoA= $\alpha = 40^\circ$ and in Mach range: $M_\infty=2\div 10$. The relations of the flow parameters (pressure and density) in upper point on leeward side pressure - P_u and density – R_u to the pressure – P_d and density – R_d in lower point on windward side in dependence on Mach number is presented on Fig. 1. The parameters relations P_u/P_d and R_u/R_d decrease

very quickly with Mach rise and are less than 10% at $M_\infty=3$ and less than 2% at $M_\infty=6$. Dependence of P_u/P_d on AoA at $M_\infty=4$ is shown in Fig. 2. Apparently that P_u/P_d diminishes quickly with AoA rise, and at $\alpha = 20^\circ$ does not exceed 15%, at $\alpha = 25^\circ$ — 7%, at $\alpha > 30^\circ$ — less than 3%. The studies confirmed validity of the Sychev's assumption about the parameter values.

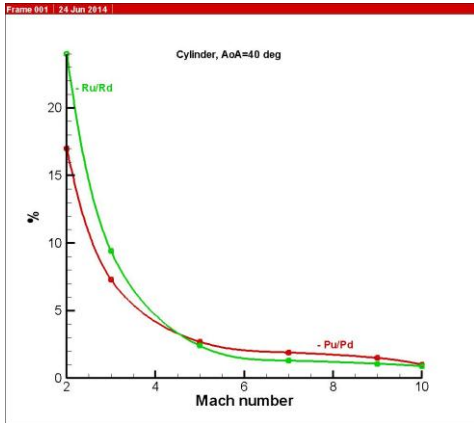


Fig. 1

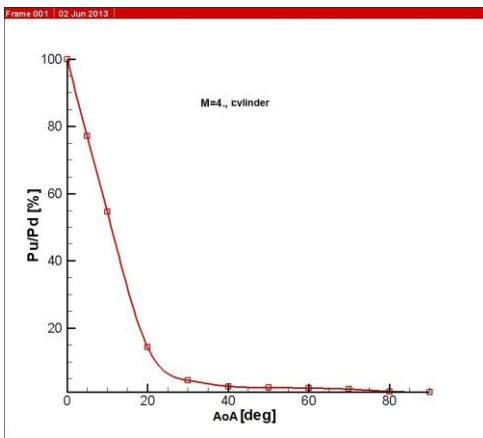


Fig. 2

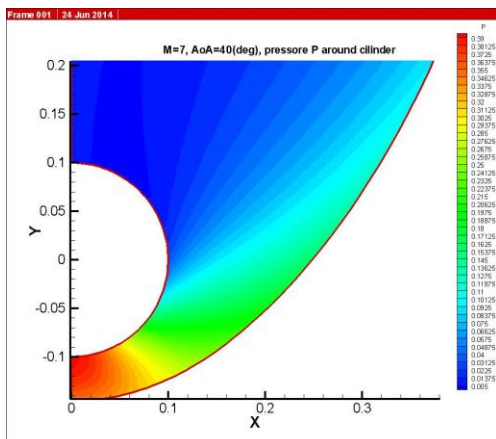


Fig. 3

Pressure field on Fig. 3 demonstrates that on major part of leeward surface pressure is substantially smaller than on windward surface.

The studies have shown the possibility to use the tool, based on Sychev's theory and Godunov-Kolgan numerical method, for the problem under consideration at $M_\infty=1.5\div 10$. One calculation regime requires about 1 minute when using the ordinary PC. If we need the pressure distribution on the body surface only, the application of engineering tool, based on Newton's method and the method of tangent wedge and cone, is quite reasonable at $M_\infty = 2\div 10$.

2.2 Methods for low Mach numbers

At low Mach numbers: $M_\infty = 0\div 2$. HSDT, Sychev's theory and Newton's method are non-applicable, moreover the contribution of leeward side flow with strong vortexes (similar to flow, shown on Fig. 11) becomes significant. In this range the RANS – solutions can be obtained with ANSYS CFX, NUMECA or similar CFD codes. Moreover, the vortex flow nonstationarity becomes essential and results into very unusual performances. Therefore, the URANS should be applied.

The reasonable question is: why don't use RANS – solutions for whole range $M_\infty=0\div 10$? There are two main causes:

- 1) One point calculation requires from a few hours to the whole day. Therefore, when it is possible (at high Mach numbers, $M_\infty=2\div 10$) it is reasonable to use more quick and robust methods;
- 2) Besides, the flow calculations at $M_\infty = 2\div 10$ meet additional problems, caused by the convergence degradation with Mach number increment. Some RANS-code developer don't guarantee the results quality when $M_\infty \geq 2.5\div 3$, even if researcher has forced the code to converge.

The applicability RANS solutions by codes NUMECA and CFX (ANSYS) for calculations at Mach numbers $M_\infty=2\div 10$ have been investigated earlier. For this purpose, the calculations of the cone with half-angle at top $\delta=10^\circ$ and zero angle of attack have been conducted in the indicated Mach number range.

The first question under consideration was the convergence of commercial RANS-codes in the indicated Mach number range. It was investigated for NUMECA-code. All calculations have been performed for the same cone, on the same mesh, with the same program parameters, including turbulence model. The results are shown on Fig. 4.



Fig. 4

Residual for density is shown here in dependence on cycles number (horizontal axis). Residual is indicated on vertical axis, and it is assumed that calculation is converged, if the residual power is less than -8 . Presented graphs show perfect convergence at $M_\infty=2$. With Mach number increment the convergence becomes worse, number of cycles, necessary to achieve residual -8 , is growing up quickly, nevertheless the convergence is achieved at $M_\infty=3, 4, 5$. But at Mach numbers $M_\infty=6, 7$ and high, the convergence didn't achieved. The residual value comes to stable level $-3 \div -3.5$ and don't go lower.

The convergence results for CFX-code for Mach numbers $M_\infty=2$ and 10 are shown on Fig. 5. These results are obtained for the same cone with half-angle at the top $\delta=10^\circ$ and zero angle of attack.

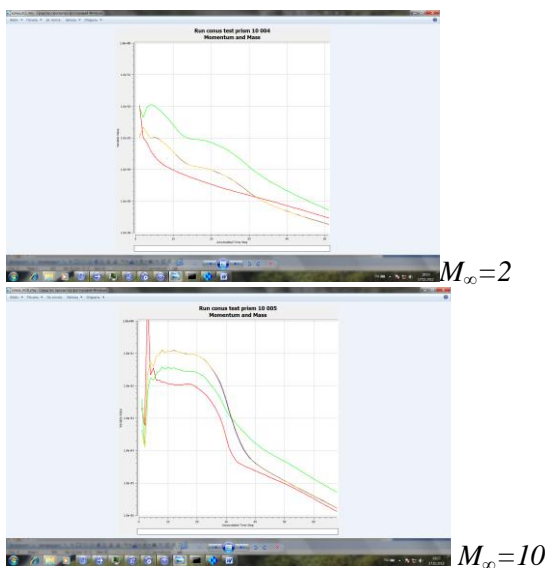


Fig. 5

These results demonstrate also the convergence reduction with Mach number increment. Nevertheless, the calculations have converged for all Mach numbers under consideration. But it is necessary to remark that the CFX-code developers guarantee the results quality up to Mach numbers $M_\infty=2.5 \div 3$. At higher Mach number, even if calculation is converged, there is no guaranty of the results rightness.

Probable reason of the RANS-code convergence reduction at Mach number rising is essential nonlinearity of equations at high supersonic velocity. In this case small velocity disturbances lead to high disturbances of other flow parameters, such as pressure, density, sound velocity, and, as a result, to worse convergence of basic iteration processes of numerical methods.

So, the RANS solution by codes NUMECA FINE/HEXA and CFX (ANSYS) have been used for low Mach number calculations ($M_\infty \leq 2$) only. Mathematical models of configurations have been created by SolidWorks, than geometry have been exported to the corresponding codes interfaces (HEXPRESS for NUMECA FINE/HEXA and ICEM for CFX).

3 Calculations

3.1 Considered configurations

Two axisymmetric configurations have been considered in this paper, mathematical models are presented on Fig. 6a and 6b.

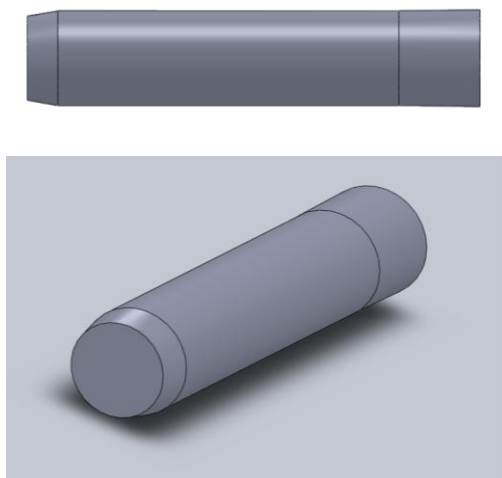


Fig. 6a Configuration 1

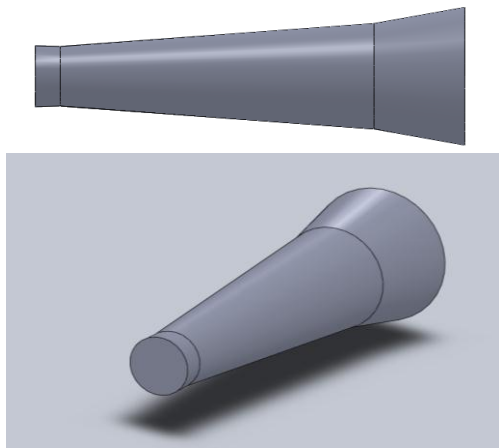


Fig. 6b Configuration 2

3.2 Calculation results

3.2.1 Low Mach numbers

Calculations for configuration 1 have been performed at $M_\infty = 0.6, 1.15, 1.5, 2$ for flight conditions, corresponding to altitude $H = 10km$.

Calculations for configuration 2 have been performed at $M_\infty = 0.15$ ($H = 0$), 0.9 ($H = 10km$), 2 ($H = 10km$).

AoA for both configurations: $\alpha = 0, 15^\circ, 30^\circ, 45^\circ, 60^\circ, 75^\circ, 90^\circ, 105^\circ, 120^\circ, 135^\circ, 150^\circ, 165^\circ, 180^\circ$.

In NUMECA code was used the hexagonal unstructured grid with prismatic boundary layer, total sells number for half-model is $2.5 \cdot 10^6$. Grids for configurations 1 and 2 are shown by Fig. 7a.

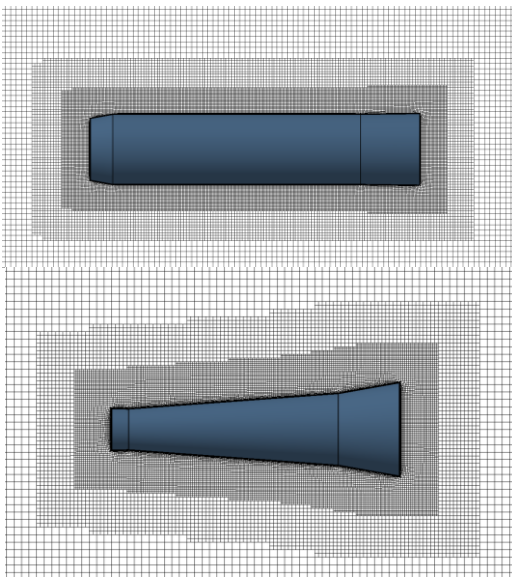


Fig. 7a NUMECA calculation grids for configurations 1 and 2

The Spalart-Allmaras turbulence model was used in NUMECA code, which provide sufficient solution accuracy and stability.

Unstructured numerical grid with $2 \cdot 10^6$ sells for half-model used for ANSYS CFX calculations is shown by Fig. 7b for both configurations 1 and 2.

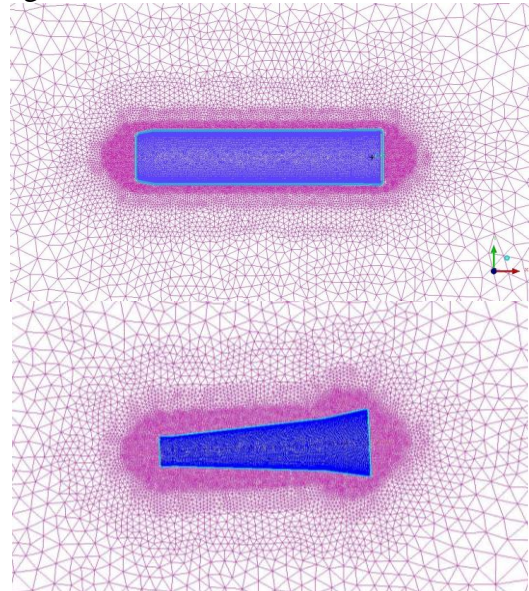


Fig. 7b ANSYS CFX calculation grids for configurations 1 and 2

Aerodynamic coefficients: C_x – drag coefficient, C_y – lift coefficient, m_z – longitudinal moment coefficient, X_d – center of pressure coordinate for buster configuration 1 in the body coordinate system are shown on Fig. 8-10 in dependence on AoA at $M_\infty = 0.6, 1.5, 2$. Characteristics for all low Mach numbers are calculated by NUMECA and ANSYS CFX codes. For $M_\infty = 1.5, 2$. The results of NINA package are shown also.

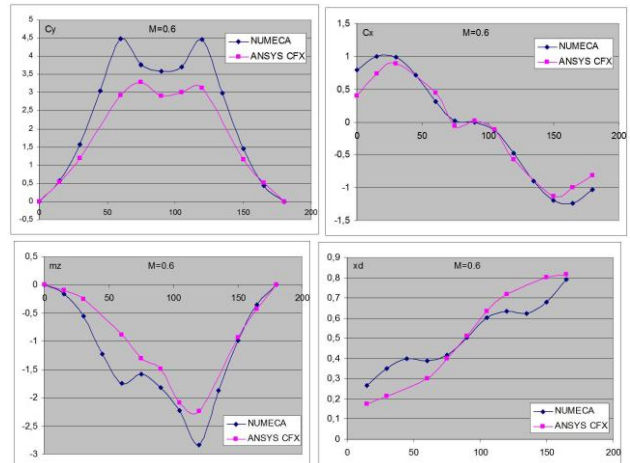


Fig. 8 Configuration 1, $M_\infty = 0.6$

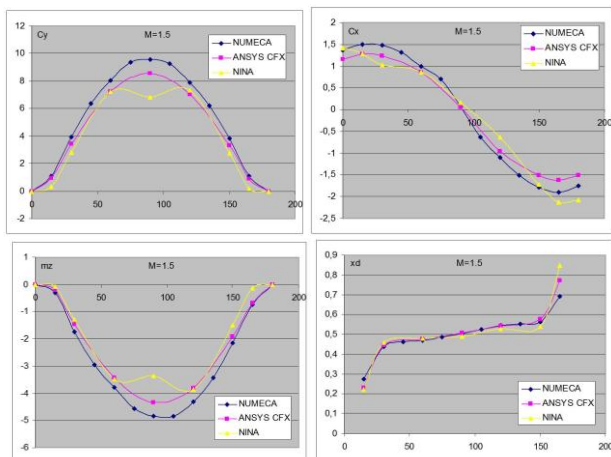


Fig. 9 Configuration 1, $M_\infty = 1.5$

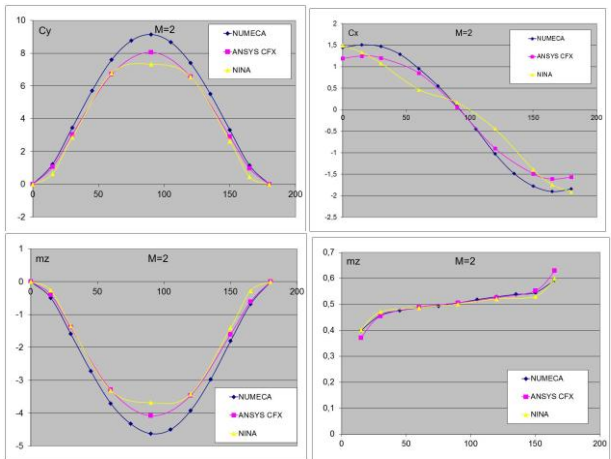


Fig. 10 Configuration 1, $M_\infty = 2$

The moment coefficients are calculated relative to the center of leading face ($x=0$).

Main peculiarities of low Mach regimes are essentially nonlinear features with local maximum and minimum points at high AoA. For example at $M_\infty = 0.6$, $\alpha = 60^\circ$ and 120° . It can be explained by the strong vortex presence on the body leeward side, which leads to the rarefaction on the upper body side and, consequently to the normal force increase.

Flow field around body configuration 1 at $M_\infty = 0.6$, $\alpha = 60^\circ$ is shown on Fig. 11. It demonstrates the strong vortex structure in the middle of the leeward side.

$$M_\infty = 0.6 \quad \alpha = 60^\circ$$

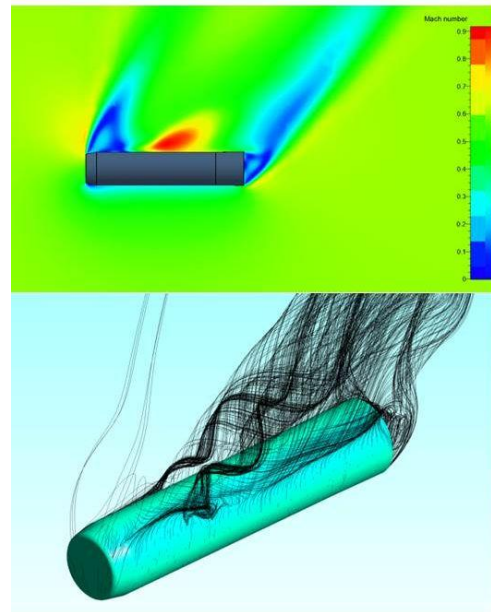


Fig. 11 Flow field for configuration 1

With AoA increase this vortex fails, the rarefaction decreases and the normal force decrease. Flow field around body configuration 1 at $M_\infty = 0.6$, $\alpha = 90^\circ$ is shown on Fig. 12. The pictures demonstrate that vortex structure is less strong and the flow is close to the flow around cylinder.

$$M_\infty = 0.6 \quad \alpha = 90^\circ$$

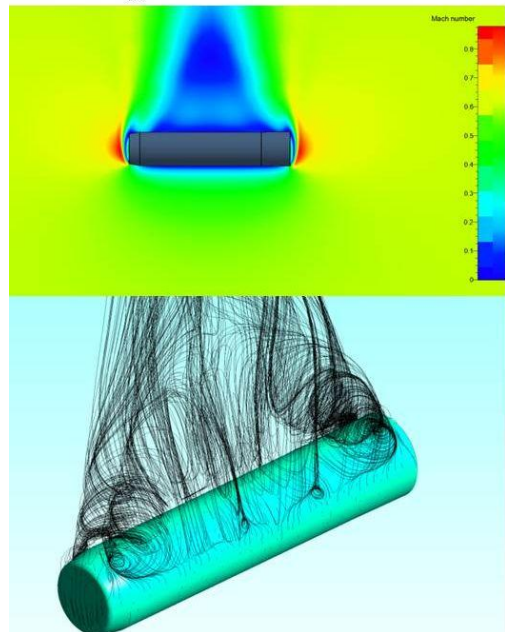


Fig. 12 Flow field for configuration 1

NUMERICAL INVESTIGATIONS ON THE SLENDER AXISYMMETRIC BODIES AERODYNAMICS IN WIDE RANGE OF MACH NUMBERS AND ANGLES OF ATTACK FROM 0° TO 180°

Flow fields around body configuration 1 at $M_\infty = 0.6$, and various AoA $\alpha = 4^\circ \div 90^\circ$ are shown on Fig. 13.

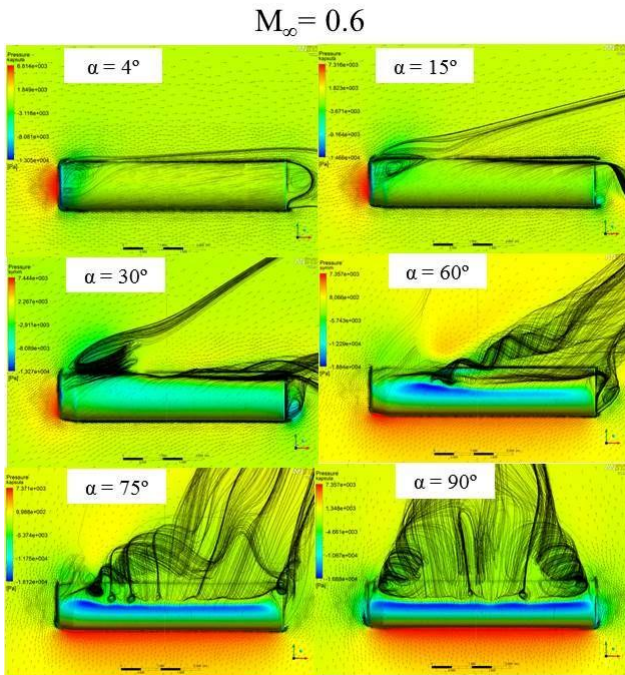


Fig. 13 Flow fields for configuration 1

Aerodynamic coefficients C_x , C_y , m_z , X_d for buster configuration 2 in body coordinates system are shown for $M_\infty = 0.15, 0.9, 2$ on Fig. 14-16.

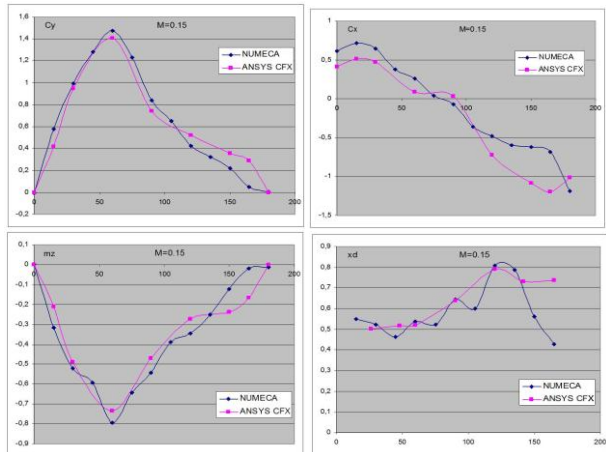


Fig. 14 Configuration 2, $M_\infty = 0.15$

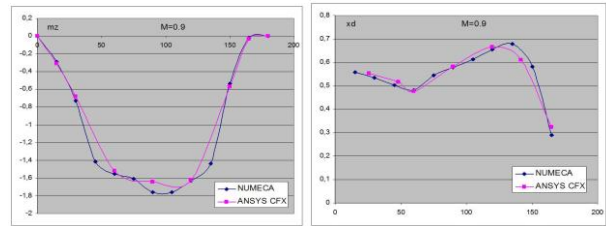
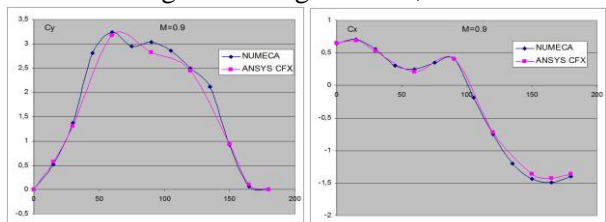


Fig. 15 Configuration 2, $M_\infty = 0.9$

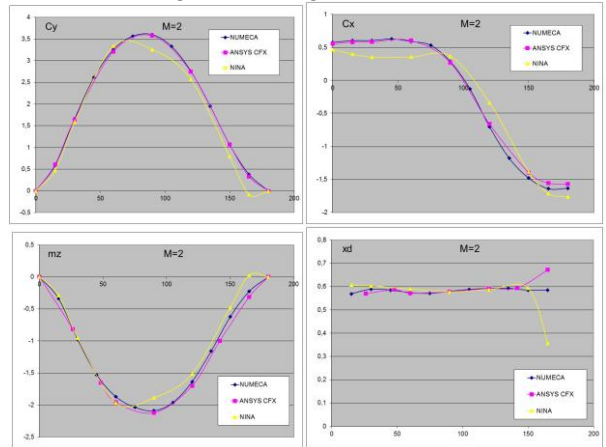


Fig. 16 Configuration 2, $M_\infty = 2$

Configuration 2 has relatively big bottom side, which causes the complex vortex structure. In this case the flow after trailing part can become unsteady at high AoA and make calculations much more difficult. Unstationarity influence becomes stronger at low Mach numbers and can decrease the results accuracy for $M_\infty = 0.15$.

3.2.2 High Mach numbers

As it is demonstrated above, the results of quite different numerical approaches are reasonable close to each other for the upper boundary of low Mach numbers range: $M_\infty = 1.5, 2$, (Fig. 9, 10, 16).

For high Mach numbers calculations was used the method described in part 2.1. Calculations for configuration 1 have been performed for $M_\infty = 4, 6, 7$. Calculations for configuration 2 have been performed at $M_\infty = 5, 10$. AoA for both configurations: $\alpha = 0, 15^\circ, 30^\circ, 45^\circ, 60^\circ, 75^\circ, 90^\circ, 105^\circ, 120^\circ, 135^\circ, 150^\circ, 165^\circ, 180^\circ$.

Because of limitations mentioned above to use CFD methods for high Mach numbers, classical Newton's method was used to compare with results of NINA package. Some results are

demonstrated for configuration 1 on Fig. 17 - $M_\infty = 4$, Fig.18 - $M_\infty = 7$, and for configuration 2 on Fig. 19 - $M_\infty = 10$.

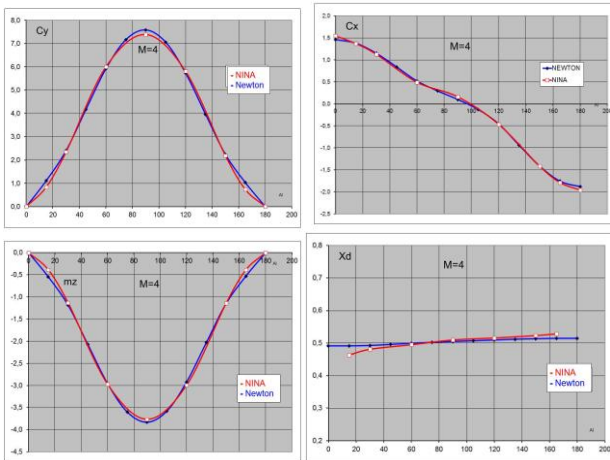


Fig. 17 Configuration 1, $M_\infty = 4$

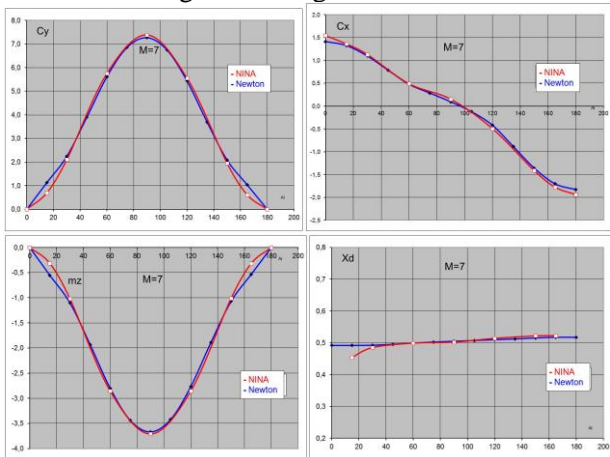


Fig. 18 Configuration 1, $M_\infty = 7$

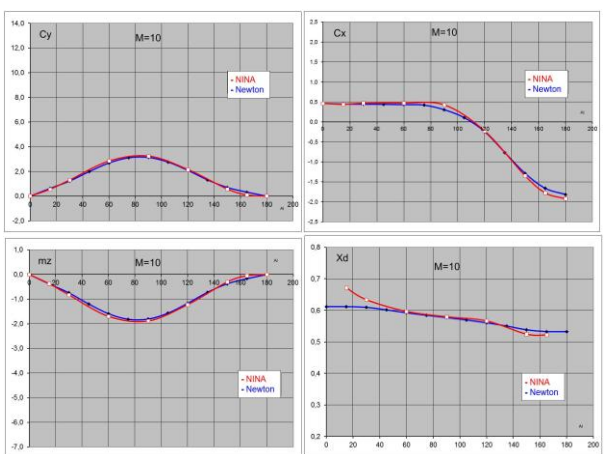


Fig. 19 Configuration 2, $M_\infty = 10$

Fig. 17-19 demonstrate that high Mach regimes have more stable features without local maximum and minimum points. It can be explained by the hypersonic stabilization – phenomena good known from classical

hypersonic theory. Vortex structure, of cause, exists on the body leeward side, but the leeward flow parameters on the upper body side are much less than parameters in strongly compressed flow on windward side. So, main input is from windward side, where flow is stable. Fig. 20 demonstrates the pressure field cross sections in the middle of configuration 1 at $M_\infty = 4$ and $\alpha = 10^\circ, 40^\circ, 60^\circ, 80^\circ$.

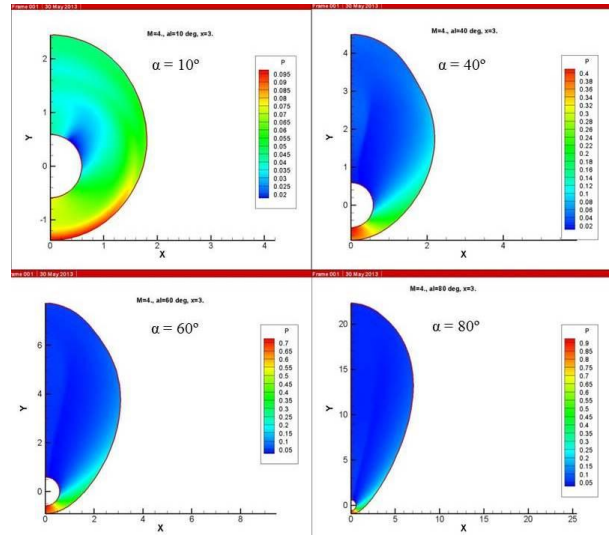


Fig. 20 Configuration 1, $M_\infty = 4$

These pictures confirm the HSDT assumptions: the pressure on the upper flow part, indicated by blue colour, is more than 10 times less than in lower flow part at $\text{AoA} > 15^\circ$. It is interesting, that Newton method results are very close to NINA package results at high Mach numbers. So, main local parameter is the body surface to the free stream direction inclination. This is right, when there is not influence from configuration parts, located upstream, for example, vortexes don't come to the body surface. It is correct for considered buster configurations.

3 Conclusions

1. The aerodynamic characteristics and the flows around slender axisymmetric bodies are investigated numerically in wide range of parameters: $M_\infty = 0. \div 10. , \alpha = 0^\circ \div 180^\circ$.
2. Calculations with various numerical, theoretical and engineering methods are conducted to determine aerodynamic characteristics of two buster configurations.
3. NUMECA and ANSYS CFX commercial codes have been used for calculations at

low Mach numbers $M_\infty = 0 \div 2$ and $\alpha = 0^\circ \div 180^\circ$. On upper boundary of Mach range was also used NINA code.

4. Numerical package NINA, based on HSDT and Godunov-Kolgan method was used for calculations at high Mach numbers $M_\infty = 1.5 \div 10$ and $\alpha = 0^\circ \div 180^\circ$.
5. Numerical investigations have demonstrated the Sychev's assumptions validity for considered regimes and configurations.
6. Essentially nonlinear features with local maximum and minimum points at high AoA have been obtained in the low Mach number range.
7. Hypersonic stabilization is observed in high Mach number range for considered configurations.
8. Different numerical methods results demonstrate acceptable coincidence.

distribution of this paper as part of the ICAS 2014 proceedings or as individual off-prints from the proceedings.

References

- [1] Hayes W and Probstein R. *Hypersonic flow theory*. Academic Press. New York and London 1959.
- [2] Sychev V. Three-Dimensional Hypersonic Gas Flow Past Slender Bodies at High Angles of Attack. *Journal of Applied Mathematics and Mechanics*, V.24, No.2, 1960.
- [3] Godunov S, Zabrodin A, Ivanov M, Krajko A and Prokopov G. *Numerical solution of multidimensional gasdynamics problems*. Moscow, Nauka, 1976.
- [4] Voevodenko N and Panteleev I. Numerical simulation of supersonic flows near any-swept wings in a large angle-of-attack range by Sychev's theory. *Fluid and Gas Mechanics*, No.2, 1992.

8 Contact Author Email Address

Mailto: nvoevodenko@yandex.ru

Copyright Statement

The authors confirm that they, and/or their company or organization, hold copyright on all of the original material included in this paper. The authors also confirm that they have obtained permission, from the copyright holder of any third party material included in this paper, to publish it as part of their paper. The authors confirm that they give permission, or have obtained permission from the copyright holder of this paper, for the publication and